Materials Science-Poland, 40(3), 2022, pp. 93-111
http://www.materialsscience.pwr.wroc.pl/
DOI: 10.2478/msp-2022-0035

sciendo

Application possibilities of scanning acoustic microscopy in the assessment of explosive welding

Marcin Korzeniowski[1,*], Beata Białobrzeska[2], Anna Lewandowska[3]

[1]Department of Metal Forming, Welding and Metrology, Faculty of Mechanical Engineering, Wrocław University of Science and Technology, Wybrzeże Wyspiańskiego 27, 50-370 Wrocław

[2]Department of Vehicle Engineering, Faculty of Mechanical Engineering, Wrocław University of Science and Technology, Wybrzeże Wyspiańskiego 27, 50-370 Wrocław

[3]Student of Mechanical Engineering and Machine Building, Faculty of Mechanical Engineering, Wrocław University of Science and Technology, Wybrzeże Wyspiańskiego 27, 50-370 Wrocław

The last two decades have brought stable and impressive development accompanied by the industry acceptance of the use of high energy techniques based on energy obtained from explosive detonation energy. Such manufacturing processes are not only commercially viable, but also allow complex product shapes and unique combinations of metal sheets in terms of materials to be obtained; they enable the creation of composites which cannot be obtained by other conventional methods. Plated sheets are composed of a base material and a thinner plating material layer. An essential aspect in the validation of explosive welding is the quality control of joints made using this technology. The basic control methods are destructive tests – mainly metallographic, which reveal the microstructure at the connection boundary. Non-destructive tests, used in industrial practice, are classical, normalised ultrasonic tests of welding joints, conducted in accordance with ISO 17640:2017 and ISO 11666:2018 standards. Due to the relatively low thickness of the explosion-tested layers (2 mm and 3 mm single layers), which is the object of this study, assessing them using widely available ultrasonic techniques is limited. According to current scientific studies, the application of the scanning acoustic microscopy (SAM) is a prospective non-destructive method allowing for the qualitative and quantitative assessment of the continuity of the metallic connection on the contact surface of two materials. This paper presents the results of research on the quality of clads, welded explosively using a non-destructive research technique, namely SAM, verified with metallographic tests.

Keywords: *non-destructive testing, scanning acoustic microscopy, cladding, explosive welding, metallography*

1. Introduction

Despite the fact that, in comparison with traditional welding techniques, explosive welding is a relatively new method, it can be certainly said that the first explosive welds appeared as early as the 80s of the 19th century, i.e., at the time firing at a high speed started and missiles would hit metal targets [1]. Subsequently, during World War I, the first observations were made to be later used as the basis for developing new applications of this process. It was discovered that missile shards embedded in armour were welded to it. In the process, high temperature, required in conventional welding methods, was of no significance. Therefore, it was found that the connecting effect resulted from the effect of the explosion power on shards. This phenomenon later became the subject of numerous laboratory studies. However, in spite of interesting results obtained in the first experimental tests [2] in the 40s of the 20th century, discussed, e.g., by Lavrentiev in 1947, their potential was not fully appreciated. Subsequent publications on explosive welding appeared at the end of the 1950s [1], and in 1964 the method was patented by DuPont [3], while the process itself was then called Detaclad.

Explosive welding is one of the protective metal cladding techniques used on metal substrates. Joints are obtained as a result of explosive detonation leading to the collision of connected elements at high speeds. The obtained joints are characterised by a wavy structure, high strength, and

* E-mail: Marcin.korzeniowski@pwr.edu.pl

© Korzeniowski et al. 2022. This is an open access article distributed under the Creative Commons Attribution-NonCommercial-NoDerivatives 4.0 License. (http://creativecommons.org/licenses/by-nc-nd/4.0/)

increased corrosion resistance. The method allows heteronymous materials whose joining using conventional methods is either difficult or even impossible to be combined [4], for instance, steel and aluminium [5–7], steel and titanium [8–13], nickel and aluminium alloys [14], iron and copper [15, 16], aluminium, copper and magnesium [17–19], copper, titanium and steel [20–24], aluminium and copper [25–27] and also metallic glass [28–30]. Moreover, this process enables joining large surfaces owing to the possibility of distributing high density energy through an explosion [31]. Despite the fact that the detonation of explosive material generates a significant amount of heat, it does not have enough time to transfer this heat inside the base metal, which undoubtedly would have an adverse effect on its structure. The very joint with wavy morphology is a complex system of nanomaterial amorphic compounds, frequently characterised by nonstoichiometric composition [32]. The creation of an amorphic layer in the joint zone was observed in various combinations of metals and it is interpreted as the basic explosive welding mechanism [33].

The mechanism of joint creation in explosive welding is a complex issue. It is considered that it is the combined effect of a few simultaneous processes. The most important ones are: self-cleaning of the surface, the so-called streaming, wave formation, plastic deformation, heat processes and effect of tensile stress [4]. Obtaining joints with required properties is possible only when oxides and absorbed gases present on the surface of the joined materials are removed. In the case of explosive welding, this can be ensured by streaming. This phenomenon consists of discarding thin surface layers of both welded plates, including the contaminants and metal particles included in them, at a high speed. These particles, depending on the collision angle, are either thrown outside the welding area, or they settle in the material of the welded elements [33]. Simultaneously, along with streaming on the surface layers of welded plates, strong plastic deformation occurs. The resulting conditions allow pure metals to move closer to each other at the collision place and create a metallic bond.

In flat joints, plasma stream is completely pushed out of the joint area. In the case of wavy joints, only a part of the stream is removed from the welded area, and the other part is trapped in the joint in the form of swirls – remeltings. The presence of a large number of remeltings in joints has an adverse effect on the joint and a negative influence on its quality [34]. Apart from remeltings, some other critical defects are all sorts of cracks and stratifications. However, due to the particular shape of the joint obtained using explosive welding, it is extremely difficult to efficiently assess these defects using any of the non-destructive tests. Such attempts were made using resonance acoustic spectroscopy by Akbari-Mousavi et al. [12]. Owing to the use of a suitable correction of inter-phase mass and elastic constants used in wave dispersion, perfect compliance between the measures and calculated resonant frequencies of the system was obtained. Ultrasonic tests were immediately used to assess input materials before the joining process [35]. However, it should be noted that the conducted research regarded the effect of high-frequency acoustic waves accompanying the explosive welding process on the quality of the obtained joint. Kuz'min et al. [36] observed that in a copper-aluminium joint created in a process in which explosive welding was accompanied by ultrasonic waves, waviness was decreased twofold and shear strength increased by 15–20% in comparison with the joints created without ultrasonic waves.

One of the non-destructive measurement techniques that could be applied to assess the quality of explosively welded joints is scanning acoustic microscopy (SAM), which has been successfully used to characterise construction materials (metallic, plastic and ceramic ones) and biological tissues for many years. SAM is a type of automated ultrasonic test using a manipulator (moving a tested object of a head) and focusing ultrasonic waves with acoustic lenses. In this way it is possible to obtain higher measurement resolution and the magnifying effect of the analysed objects, in comparison with conventional ultrasonic equipment. SAM uses ultrasonic waves in frequency ranges approximating single gigahertzes [37]. Contrary to classical ultrasonic measuring techniques, transducers

are equipped with the so called acoustic lenses, focusing an ultrasonic wave beam on the point referred to as the focus, which allows increasing measurement resolution and obtaining the effect of image magnification. The use of SAM in fundamental research and industrial applications may be an alternative and a supplementary technique for the currently used microscopic techniques (light microscopy, SEM) and X-radiation tests (classical roentgen tests and roentgen computer tomography). The employment of advanced signal processing algorithms and images allows not only to visualise structural discrepancies (e.g., cracks or voids), but also material properties (Young modulus, Kirchoff modulus, Poisson coefficient) [37]. In Ref. [38], the possibilities of porosity assessment in padding welds made using the plasma powdered arc method are presented. It was found that the use of ultrasonic waves in the range of 30–110 MHz allows the efficient detection of pores. Xiao et al. [39] used SAM to assess the nucleus diameter of hybrid welds made using a hybrid process: resistance welding and adhesive bonding. Kubit et al. [40] used SAM to assess the quality of thin-wall joints made by Friction Stir Spot Welding (FSSW); the results of their research were presented using a C-Scan presentation. The problem of detecting subsurface defects has been extensively discussed by Li et al. [41]. The authors claimed that the use of digital filter adaptive algorithms employing morphological operations of image processing allow the increase of the detection efficiency of subsurface defects whose detectability is usually hindered by the so called dead zone. SAM using tomographic acoustic micro imaging (the so called TAMI technique) in the C-scan mode was used by Zhua et al. [42] to determine the morphology and depth of corrosion pits in 7050 aluminium alloy. Also, the development of electrical cell manufacturing technology implies the necessity of continuous monitoring. In Ref. [43], the results of cell tests conducted using SAM are presented. The results show its wide application potential and efficiency in the estimation of internal defects. Trends in SAM development are discussed in depth by Arakawa et al. [44]. That paper presents an ultrasonic device with a transducer made of ZnO, equipped with two acoustic lenses with aperture radii of 1.0 mm and 0.5 mm. The authors performed an extensive numerical analysis which turned out to be very useful in the evaluation of wave energy losses at set frequencies. Another advantage of a scanning acoustic microscope is its ability to detect discontinuity <1 μm and measure the depth of internal layers [45].

The above examples allow concluding that SAM is one of the most modern ways of using ultrasonic waves. It enables the visualisation of the internal structure of a material without the necessity to destruct and etch it. This is possible owing to the use of point beam scanning penetrating a sample placed in water. A traditional microscope allows only the surface of the sample to be observed, while SAM makes it possible to obtain the imaging of the deeper layers of the tested material.

To date, SAM has not been applied in the research on joints obtained using the explosive welding method. However, according to current scientific studies, it is possible to use SAM for the qualitative and quantitative evaluation of such joints. This paper focuses on verifying the possibility of using this kind of tests to evaluate the quality of explosively welded joints. The aim of the research was to investigate the application possibilities of SAM for quality assessment and quantitative flaw evaluation in explosive welding joints. In the analysis, presentations A, B and C-scan were used as ultrasonic signals. The obtained results were verified using metallographic tests.

2. Materials and methods

The following materials were used in the research: construction steel P355NH, steel grade D, super duplex steel SAF 2504, Inconel 625, aluminium alloys 1050 and 5083, and titanium grade 1. The structure of the materials is shown in Figure 1.

In explosive welding, there are two basic joining mechanisms that differ in the orientation of the flying plate (upper, plated sheet) relative to the base one. The plated sheet can be positioned parallel or at an angle to each other. In practice parallel arrangement is most often used. This approach

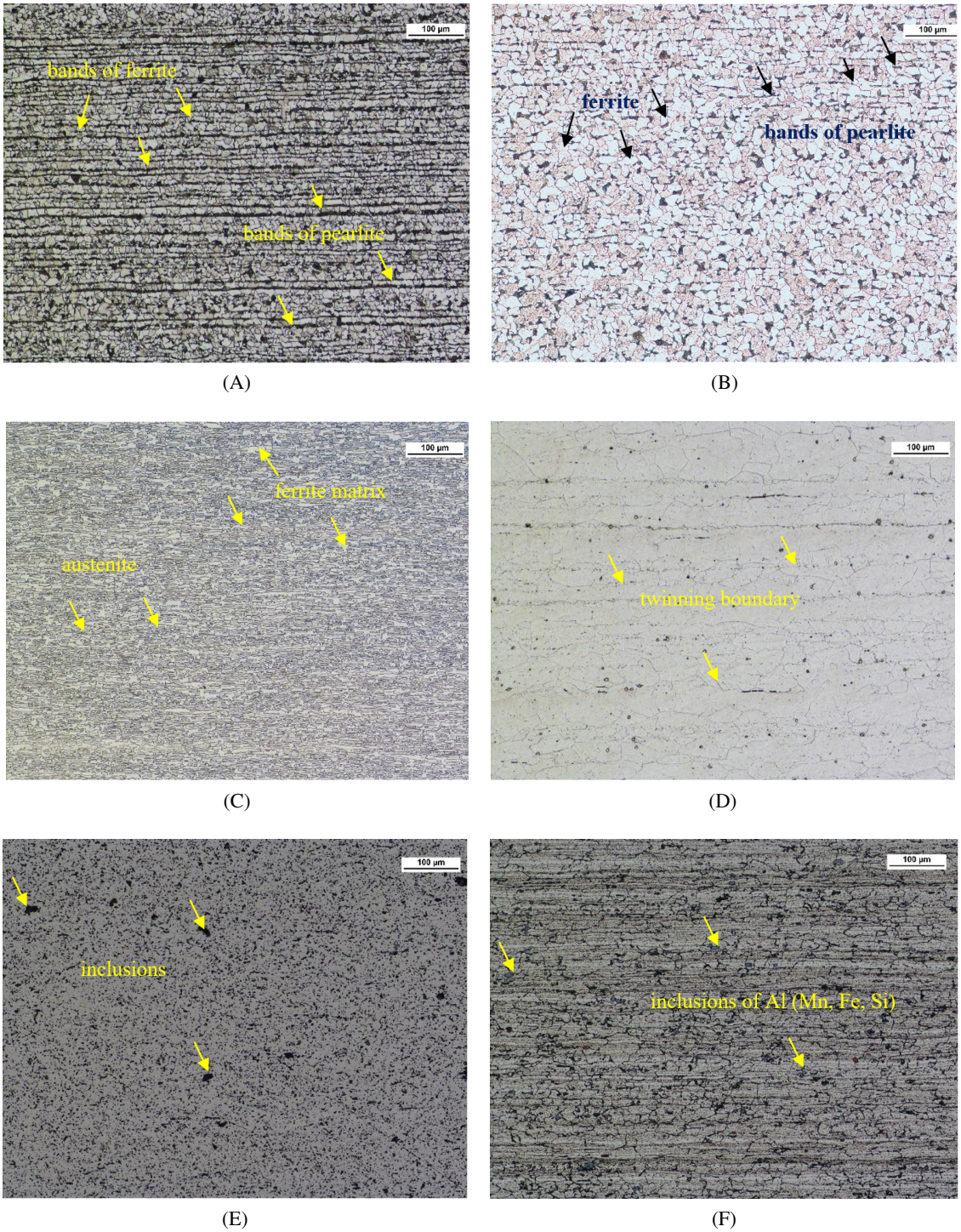
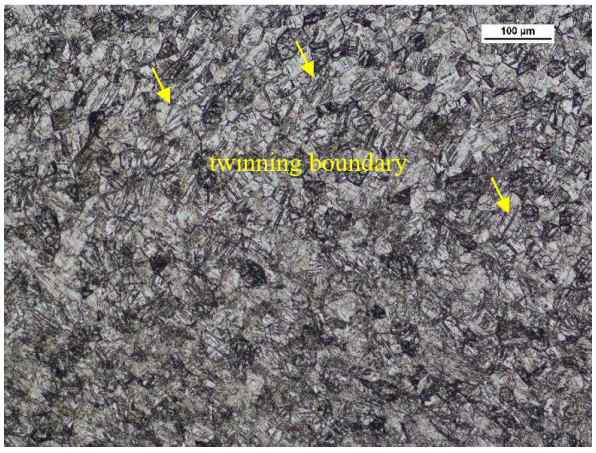


Fig. 1. Structure of analysed materials: **(A)** steel P355NH, visible ferrite and pearlite bands; **(B)** steel grade D, visible ferrite and pearlite grains, pearlite locally shows a slight banding; **(C)** steel SAF 250, visible austenite islands in a ferritic matrix; **(D)** Inconel 625, visible austenite grains with twinning boundaries; **(E)** Al 1050, dark inclusions; **(F)** Al 5083, state after plastic deformation and annealing. Visible solution α grains and Al (Mn, Fe, Si) inclusions, inter-metallic phases of Al_3Mg_2 and texture of deformation and **(G)** titanium grade 1, visible grains with twinning boundaries. Etched state, light microscopy



(G)

Fig. 1. ...continued

has been performed during manufacturing joints. Powdered explosive has been placed on the surface of the flying plate. During detonation initiated by the detonator the flying plate gets projected toward the base plate on the solid support. The detonation front moving along the movable plate causes its constant rejection and bending which causes the joined elements to collide. As a result of the collision (when the limit collision velocity has been reached) it is possible to obtain a permanent joint. Due to the specific nature of the process conducted in cooperation with military units, detailed data on the chemical composition, the amount of the explosive, and its distribution on the surface of the flying plate are not disclosed by the sample manufacturer.

Samples with 50 mm × 50 mm dimensions were cut from four various clad plates made by 'Explomet' High Energy-Techniques Works (sheet thickness is given in parentheses). Before the ultrasonic tests, surfaces were ground to eliminate the influence of the surface irregularity state (roughness, inclusions, deformation) on the ultrasonic test results. For this purpose sandpaper grade no. 1200 was used.

1. SAF 2507 – P355NH (3 mm + 10 mm);
2. Inconel 625 – P355NH (3 mm + 10 mm);
3. Steel grade D – Ti grade 1 – Al 1050 – Al 5083 (10 mm + 2 mm + 3 mm + 10 mm).

The ultrasonic tests were conducted using a scanning acoustic microscope manufactured by OKOS. Due to various material properties, the samples were tested using various parameter settings, the common parameters were a focusing transducer frequency of 25 MHz, focus size 1 mm and focal length in water 15 mm. The samples were tested at the cladded material side (in the case of bimetals SAF 2507 – P355NH and Inconel 625 – P355NH, these were steel SAF 2507 and Inconel Inconel 625, respectively, and for four-layer platter it was steel grade D) with the C-scan presentation resolution of 100 µm on the x and y axes (C-scan is an acoustical cross-section at a set measurement depth, parallel with the tested surface, assuming that the ultrasonic wave beam cast on it is perpendicular to it). B-scan presentations (an acoustical cross-section made along a set scanning surface) were made with 50 µm resolution. The ultrasonic beam generated by the transducer was focused exactly on the joint boundary (for two-layer platters at a depth of 3 mm, for four-layer platter – 4 mm).

The microstructure observations at the sample cross-sections were made using a light microscope made by Nikon Eclipse MA200. Image recording and analysis were performed using Nikon DS-Fi2 digital cameras coupled with the microscopes and the NIS Elements software made by Nikon.

3. Results

3.1. Bimetal SAF 2507 – P355NH

The microstructure near the joint line is presented in Figure 2. The joint shows waviness characteristics (Figure 2A); moreover, it is possible to discern adiabatic shear bands (ASBs), located mainly at the wave fold, and defects in the form of remeltings occurring near the boundary of the joined materials (Figures 2A–2D). ASBs, appearing as narrow, dark, etched bands in the material microstructure, are known to be the main signs of plastic deformation location [46]. As can be seen, the observed ASBs are located parallel to the seam weld or at an angle diagonal to it. The phenomena of adiabatic shear, shear instability or the location of shear bands, which are the main determiners of

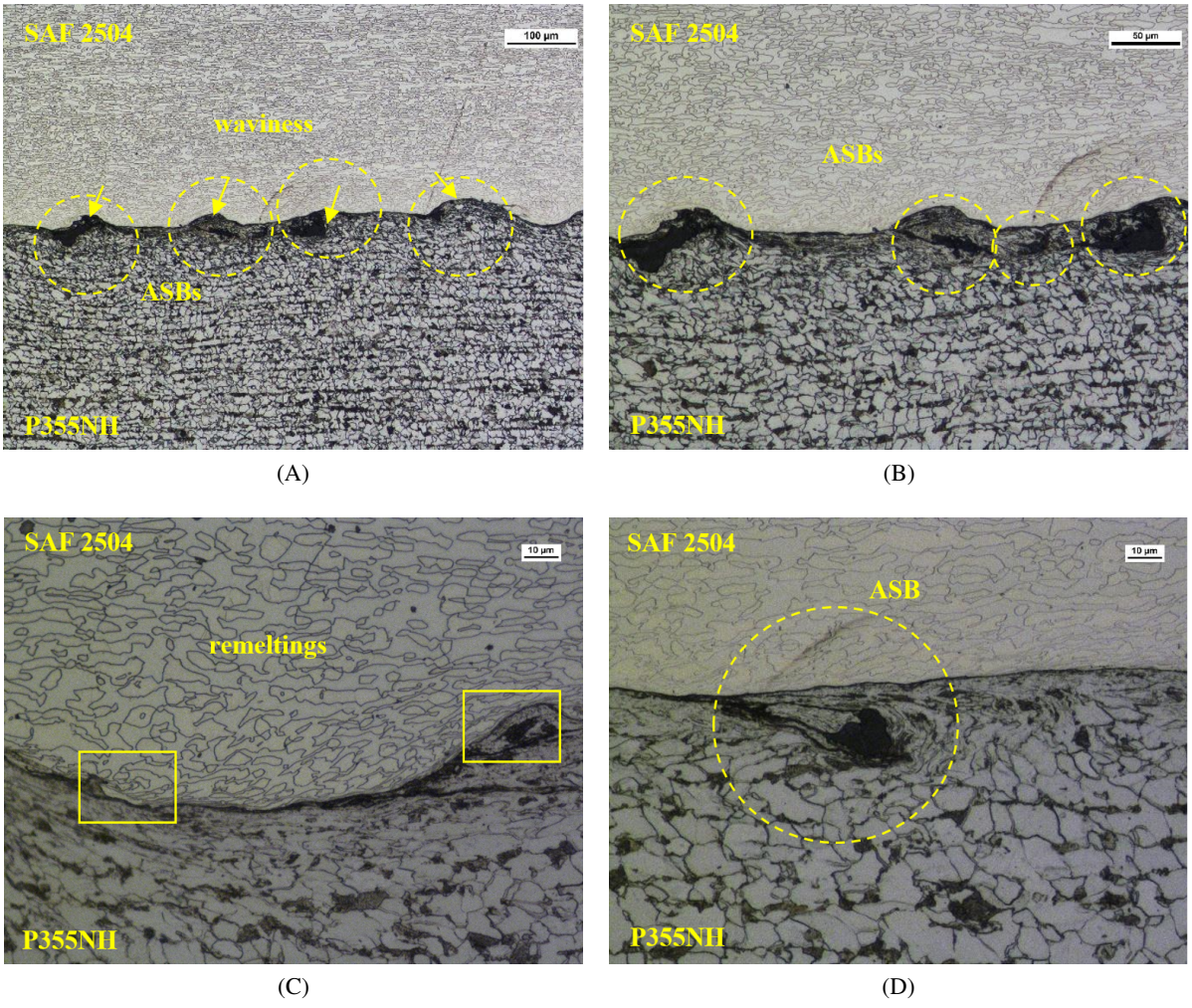
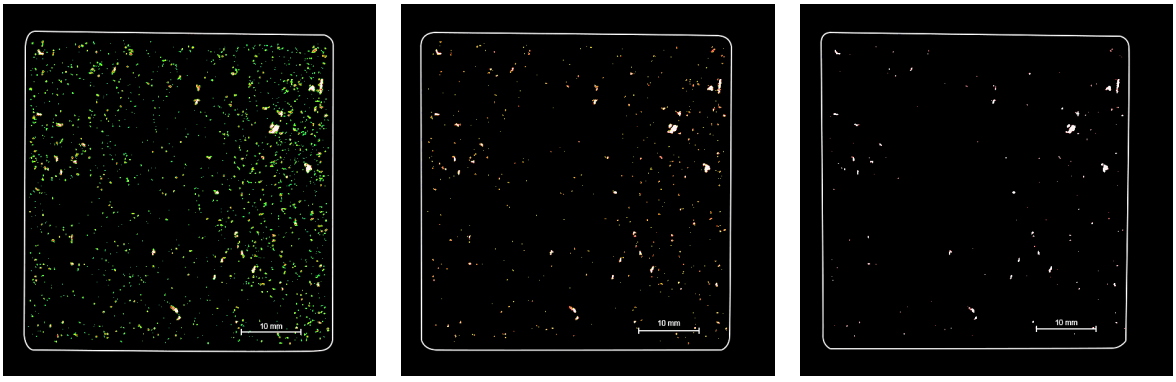


Fig. 2. Microstructure of bimetal SAF 2504 – P355NH: **(A)** 100× magnification; **(B)** 200× magnification; and **(C)** 500× magnification. Etched state, light microscopy, **(D)** 500× magnification

adiabatic shear planes, occur mainly in processes characterised by significant structure deformations of the analysed material. They result from large deformations accompanied by a dynamic recrystallisation process and the plastic flow of equiaxed recrystallised grains [47]. In addition to this, close observation of ASBs indicates the occurrence of discontinuity at the end of the bands. The phenomenon takes root from the increase in the ASB temperature. Such a high temperature decreases the strength of the material near ASBs; as a consequence, it fosters the initiation of micro-cracks by reflected tensile waves [48, 49]. Near the joint, the bandy structure of the steel partly disappeared. Some grains were deformed and elongated for the purpose of forming the characteristic wavy morphology. Near the large, elongated grains smaller grains were also observed, which can confirm the simultaneous recrystallization processes.

Figure 3 presents the ultrasonic test results of the SAF 2504 – P355NH joint in the form of a C-scan presentation for various sensitivity levels of the ultrasonic signal defined by a threshold (the so called acceptance level as per ISO 11666:2011). The threshold was set as the percentage value (45%, 65% and 85%, respectively), referred to the maximum amplitude of the recorded ultrasonic signal. When the threshold is increased, the ultrasonic



(A) (B) (C)

Fig. 3. Results of SAM C-scan ultrasonic tests, SAF 2504 – P355NH joints: **(A)** threshold 45% of reference range; **(B)** threshold 65% of reference range and **(C)** threshold 85% of reference range

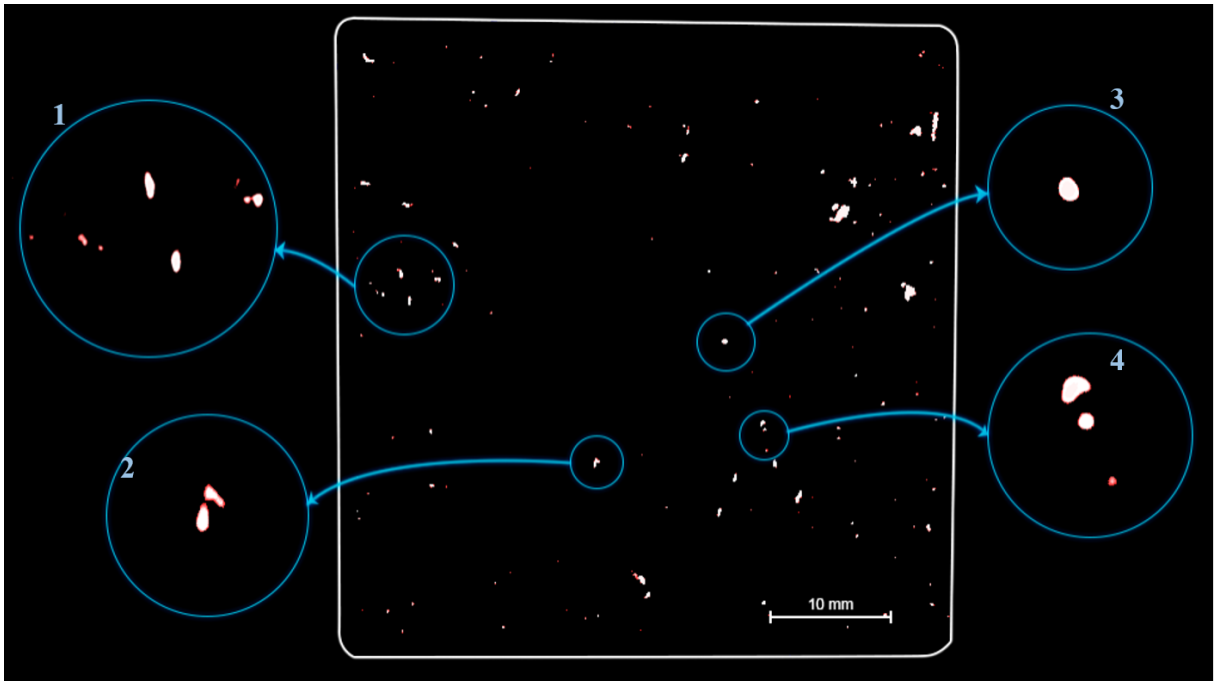
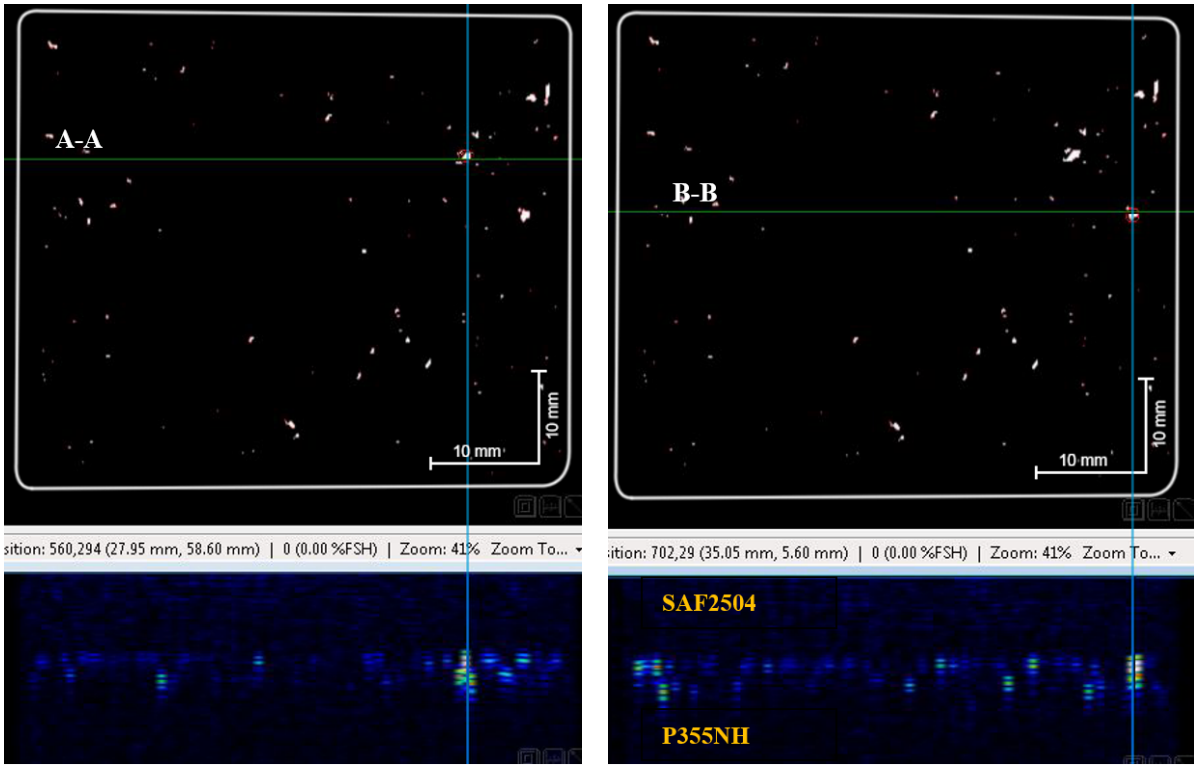


Fig. 4. Results of ultrasonic tests of SAF 2504 – P355NH joint: (1) surface 0.63 mm^2, (2) surface 0.14 mm^2, (3) surface 0.11 mm^2 and (4) surface 0.23 mm^2

signal is analysed, and the grey scale in the C-scan presentation corresponds to its amplitude values. A reduction in the threshold value results in increasing the sensitivity of the whole measurement system; it also indicates the appearance of artefacts. The gain of an ultrasonic signal is a relative value; its assumed value corresponds to 95% of the maximum amplitude scale with total signal reflection.

The discontinuity indications are visible in the form of bright points in C-scan presentation and confirm the lack of metallic continuity at a given point, which was validated by metallographic tests.

The result of the conducted research (SAM) was the confirmation of metallography, which proves that there is no joint continuity in the tested joint area. Depending on the set measurement sys-



(A) (B)

Fig. 5. C-scan and B-scan acoustic cross-sections of SAF 2504 – P355NH bimetal for two selected scanning lines: (**A**) cross section A-A and (**B**) cross section B-B

tem sensitivity level, the indications are more or less numerous. A detailed analysis was performed for the result obtained at the threshold set at 85% of the reference range, where a number of discontinuities on the joint surface were visible. Figure 4 presents the result of the C-scan ultrasonic test, with visible detailed indications starting with relatively large discontinuities on the contact surface. In the numbered areas, a magnified view of the indications is shown and the measurement of the summary area where discrepancies occurred (in mm^2).

Figure 5 presents the C-scan presentations with marked scanning lines (green straight lines in the C-scan presentation), for which it was performed an acoustic cross-section perpendicular to the surface on which a wave falls (B-scan). Along the entire width of the B-scan presentation there is a visible division line which confirms partial wave reflection, resulting from the existence of two media with different acoustic impedances (duplex type steel – low-carbon steel). Due to the fact that B-scan presentation is a variety of the A-scan presentation in the form of a two-dimensional image, in which the x axis corresponds to the linear dimension, and the y axis to the time of acoustic wave transition, it is possible to assess the depth of discontinuities (with the known sound speed in the material).

SAM, apart from A-, B- and C-scan classical visualisations, allows also the ultrasonic signals to be analysed by making acoustic cross-sections at various depth levels (the so called X-scan presentations). They are created as a result of narrowing the shift of the ultrasonic signal observation range along the time axis; following multiplication by sound speed, the signal can be transformed to distance (depth against surface).

Figure 6A presents the C-scan presentation of the examined area in the range of 2.9–3.0 mm, and

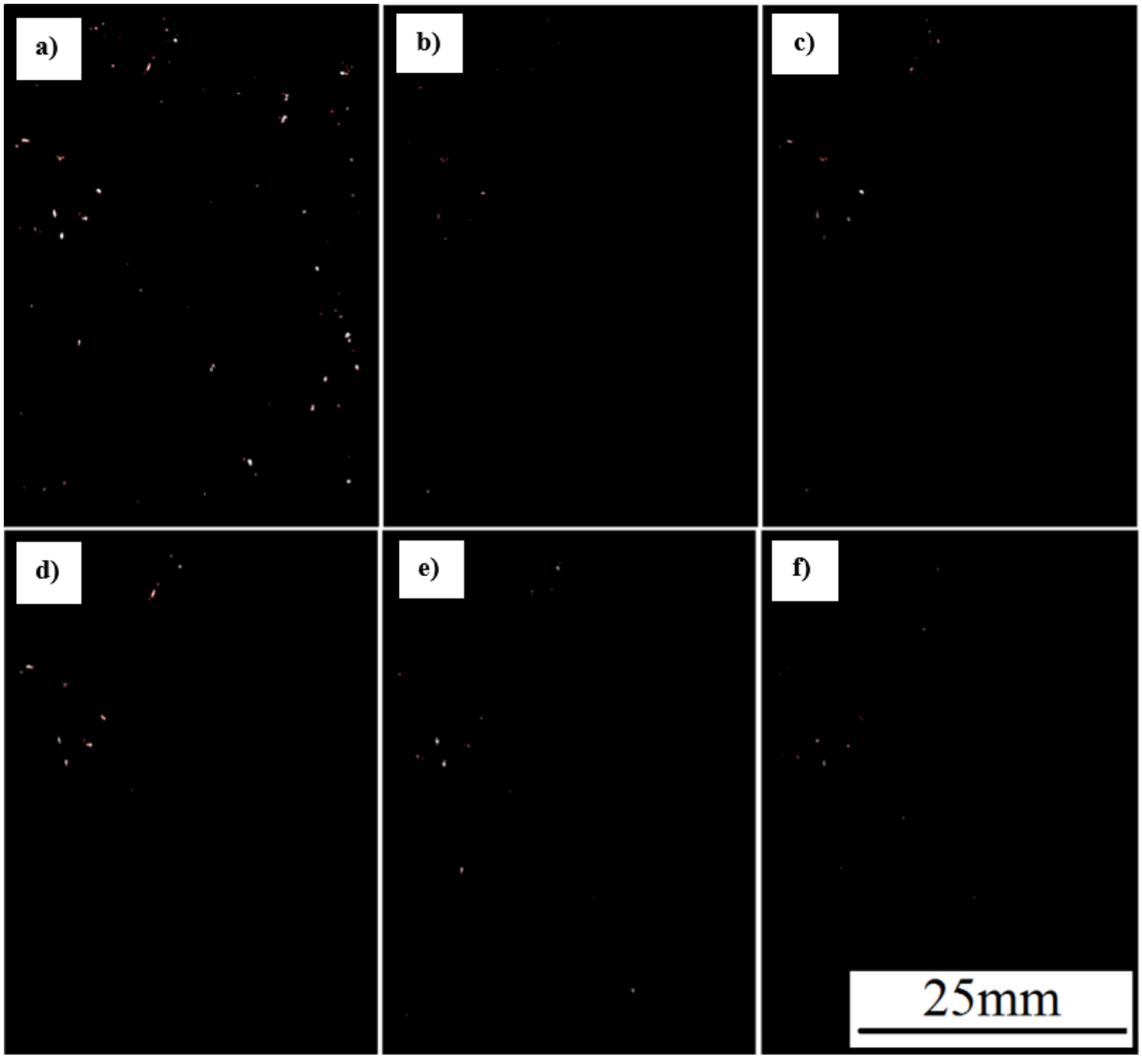


Fig. 6. X-scan presentations of SAF 2504 – P355NH joint: **(A)** C-scan registered in 2.9–3.00 mm range; **(B)** depth 2.94 mm; **(C)** depth 2.95 mm; **(D)** depth 2.96 mm; **(E)** depth 2.97 mm and **(F)** depth 2.98 mm

Figures 6B–6F at the depths of 2.94–2.98 mm, respectively. Owing to this visualisation method, it is possible to precisely determine the geometry of indications at a given depth.

3.2. Bimetal Inconel 625 – P355NH

The microstructure near the joint line is presented in Figure 7. The joint has typical features such as waviness (Figures 7A–7C), and also remeltings occur near the boundary of the joined materials (Figures 7A and 7B). Moreover, adiabatic shear bands (ASB) can be distinguished (Figures 7B–7C). The literature analysis of remeltings showed that the elements originating from Inconel 625 alloy have a higher participation than those originating from steel [50]. In the case of steel, the banded structure partly disappeared near the joint. Both steel and Inconel 625 alloy grains were deformed and elongated for the purpose of creating waves, also some grains in the wave crests were fragmented. In addition to this, a detailed analysis of adiabatic shear bands and remeltings allowed

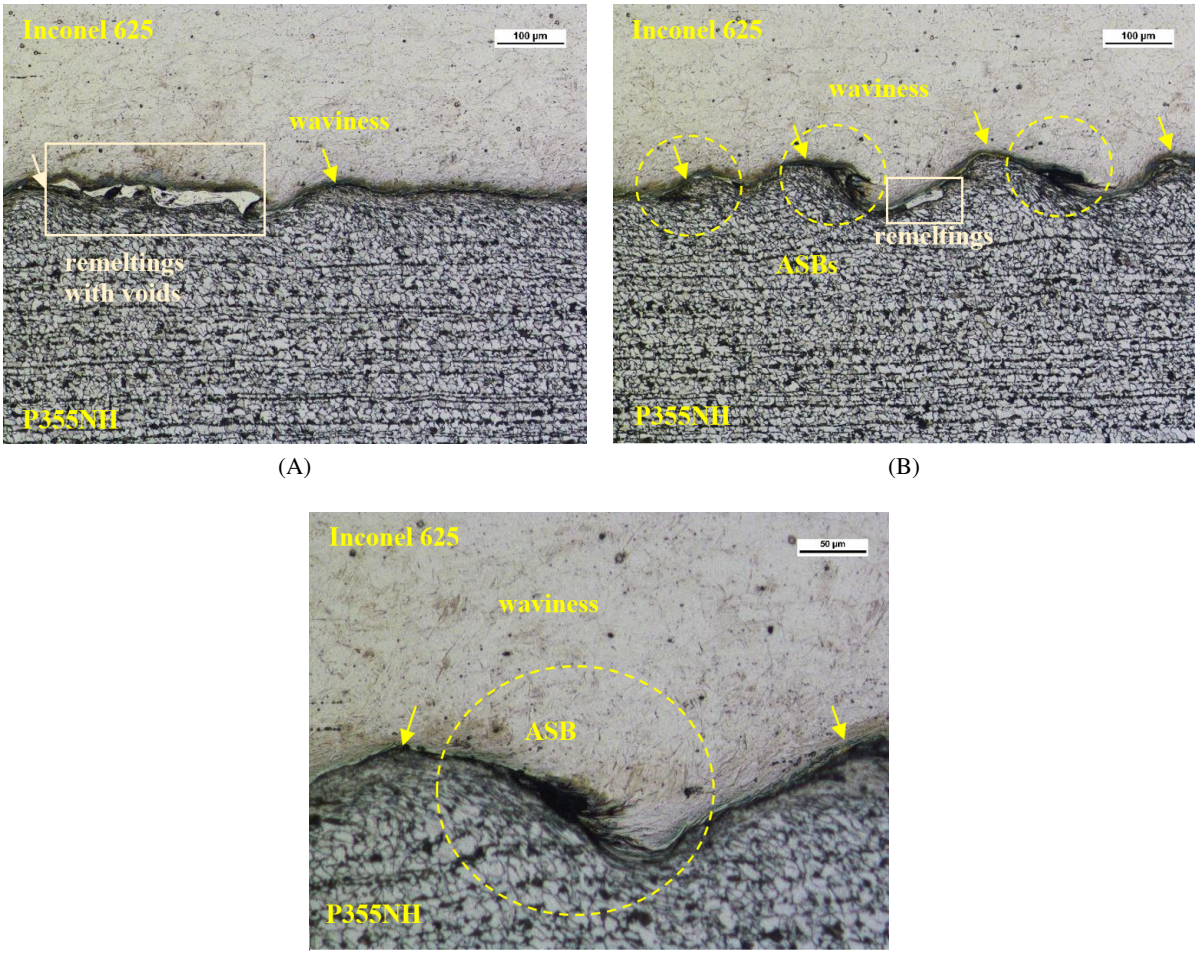


Fig. 7. Microstructure of Inconel 625 – P355NH bimetal: **(A)** magnification 100×; **(B)** magnification 100×; and **(C)** magnification 200×. Etched state, light microscopy

discontinuity in the material to be observed in the form of voids and pores.

The testing procedure of Inconel 625 – P355NH joints was analogous to that used in the case of the SAF 2504 – P355NH joint. First of all, due to the different acoustic properties of the cladded material, for the discussed joint, the gain values and the height of the registration level were adapted to the cladded material (Inconel 625). Figure 8 presents an acoustic cross-section parallel to the surface (C-Scan) along the joint line of Inconel 625 – P355NH bimetal. As a result of the conducted research, single indications which may confirm the presence of possible discontinuities and imperfections in the joint were found in the analysed sample. Four biggest discontinuities, whose areas were 1 – 0.03 mm^2, 2 – 0.09 mm^2, 3 – 0.05 mm^2 and 4 – 0.06 mm^2, respectively, were marked.

Figure 9 shows C- and B-scan presentations with corresponding B-scan presentations on selected scanning lines (horizontal green line – C-scan). The analysis of the B-Scan presentation for two scanning lines indicates that there are discontinuities on the joint line, which confirms potential imperfections in the joint.

Figure 10A shows the C-scan presentation of the examined area in the range 3.01–3.06 mm, and in Figures 10B–10F at the depth of 3.01 mm, 3.02 mm, 3.04 mm, 3.05 and 3.06 mm, respectively.

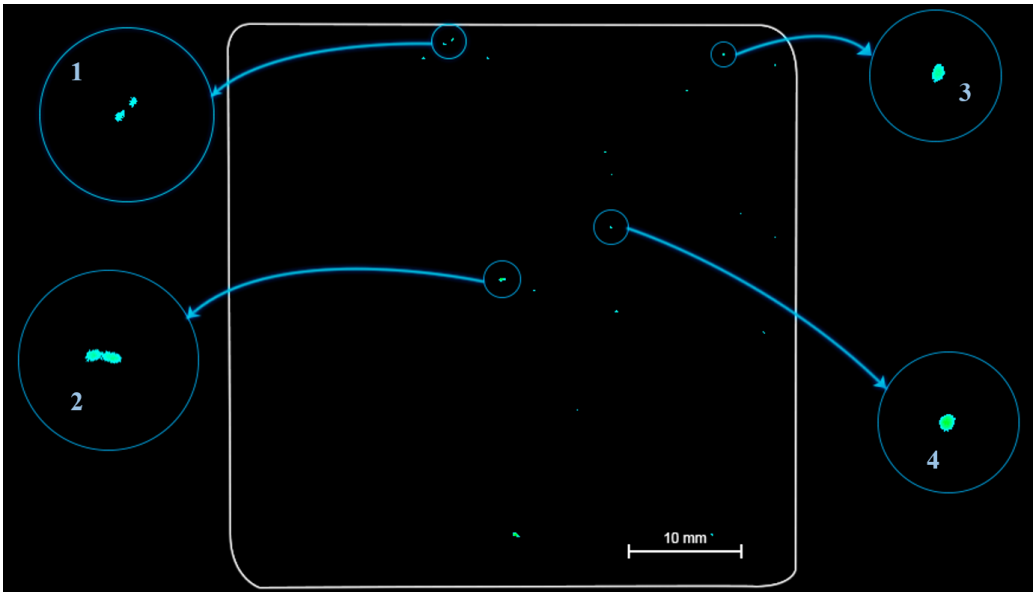
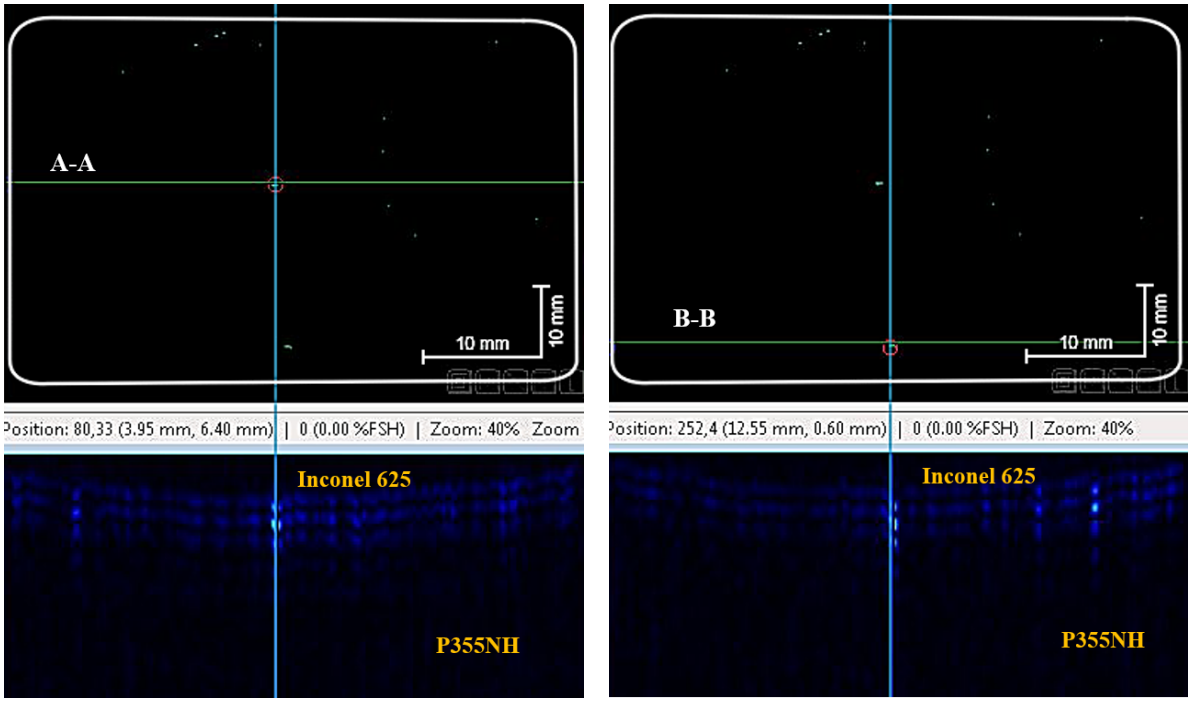


Fig. 8. Results of C-scan indications of ultrasonic tests of the Inconel 625 – P355NH joint. Close-ups of particular indications: (1) surface 0.03 mm^2; (2) surface 0.09 mm^2; (3) surface 0.05 mm^2 and (4) surface 0.06 mm^2, scanning acoustic microscope



(A) (B)

Fig. 9. C-scan and B-scan acoustic cross-sections of Inconel 625 – P355NH bimetal for two selected scanning lines: **(A)** cross section A–A and **(B)** cross section B–B

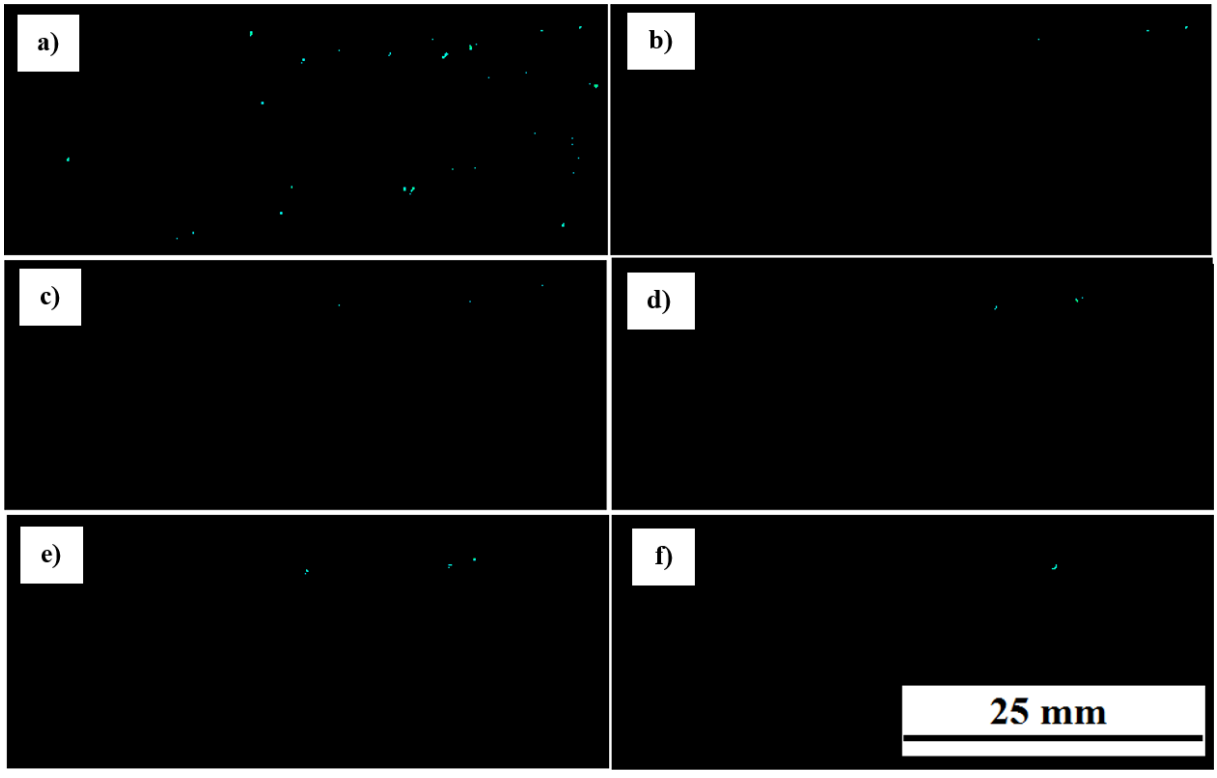


Fig. 10. X-scan presentations of Inconel 625 – P355NH joint: **(A)** C-scan registered in the range of 3.01–3.06 mm; **(B)** depth 3.01 mm; **(C)** depth 3.02 mm; **(D)** depth 3.04 mm; **(E)** depth 3.05 mm and **(F)** depth 3.06 mm

3.3. Four-layer clad plate: steel grade no. D – Ti grade 1 – Al 1050 – Al 5083

The joint of steel grade D and titanium grade 1 is presented in Figures 11A and 11B. The joint is characterised by high waviness, large areas with adiabatic shear bands and remeltings. The analysis of bands and remeltings revealed the presence of discontinuities and pores (Figure 11B). Ample literature data confirm the participation of both iron and titanium in the created remeltings in the form of metallic inclusions with stoichiometric formula Fe_2Ti and FeTi. Some researchers report amorphous phases occurring at the Ti/steel phase boundary [51–53]. Fe-Ti alloys do not have a high glass forming ability. Even when near the eutectic structure, amorphous Fe-Ti phases are rarely obtained in fast cooling experiments. Small additions of alloy elements in titanium and steel may increase the ability to create amorphous phases [54]; however, the content of alloy elements in the analysed materials is relatively low, which may be the reason for the lack of amorphous phases in the mixing zone.

The joint of titanium grade 1 and Al 1050 is shown in Figures 11C and 11D. It is characterised by lower waviness than the joint of titanium and steel. Remeltings are not so numerous and adiabatic shear lines are smaller (Figure 11D). It was shown that in the remelted zones, Ti concentration fluctuates from 17 at.% to 67 at.%, while for Al – from 33 at.% to 83 at.% [55]. The SEM/EDX analyses demonstrated that in the remelted zone structures metastable phases prevail. The chemical composition of these phases was determined to be as follows: Ti (20–70 at.%) and Al (20–70 at.%). However, the above results also indicate the presence of a wide spectrum of intermetallic phases with chemical composition very similar to that of Al_3Ti, Al_2Ti, AlTi, $AlTi_2$, and $AlTi_3$ equilibrium phases. In the case of thin remelted zones, usually observed near the central and bottom plate boundaries, the chemical composition may be directly related to equilibrium phases Al_3Ti, $AlTi_2$,

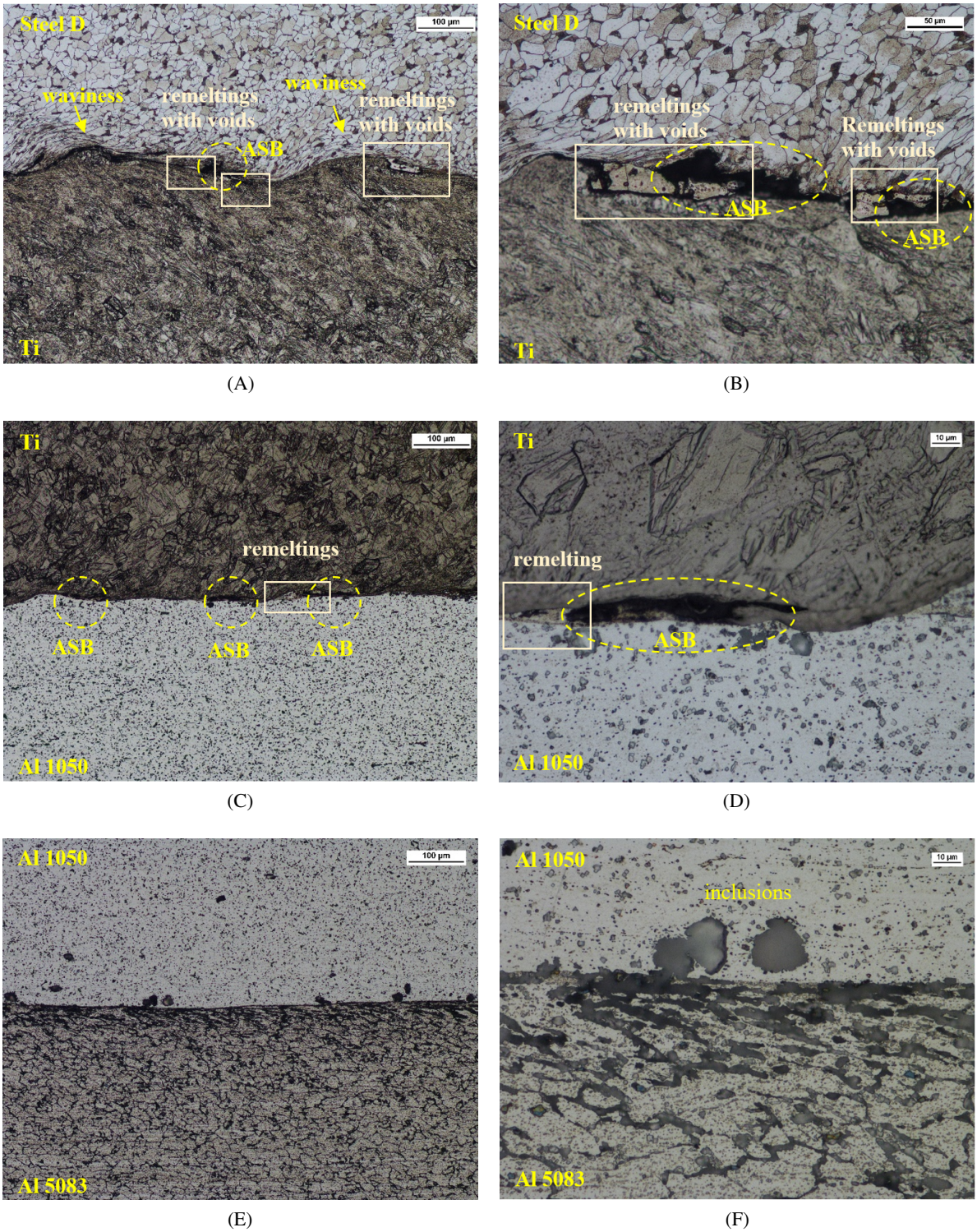


Fig. 11. Microstructure of a four-layer clad plate: steel grade D – Ti grade 1 – Al 1050 – Al 5083: **(A)** steel grade D – Ti grade 1, magnification 100×; **(B)** steel grade D – Ti grade 1, magnification 200×; **(C)** Ti grade 1 – Al 1050, magnification 100×; **(D)** Ti grade 1 – Al 1050, magnification 500×; **(E)** Al 1050 – Al 5083, magnification 100× and **(F)** Al 1050 – Al 5083, magnification 500×. Etched state, light microscopy

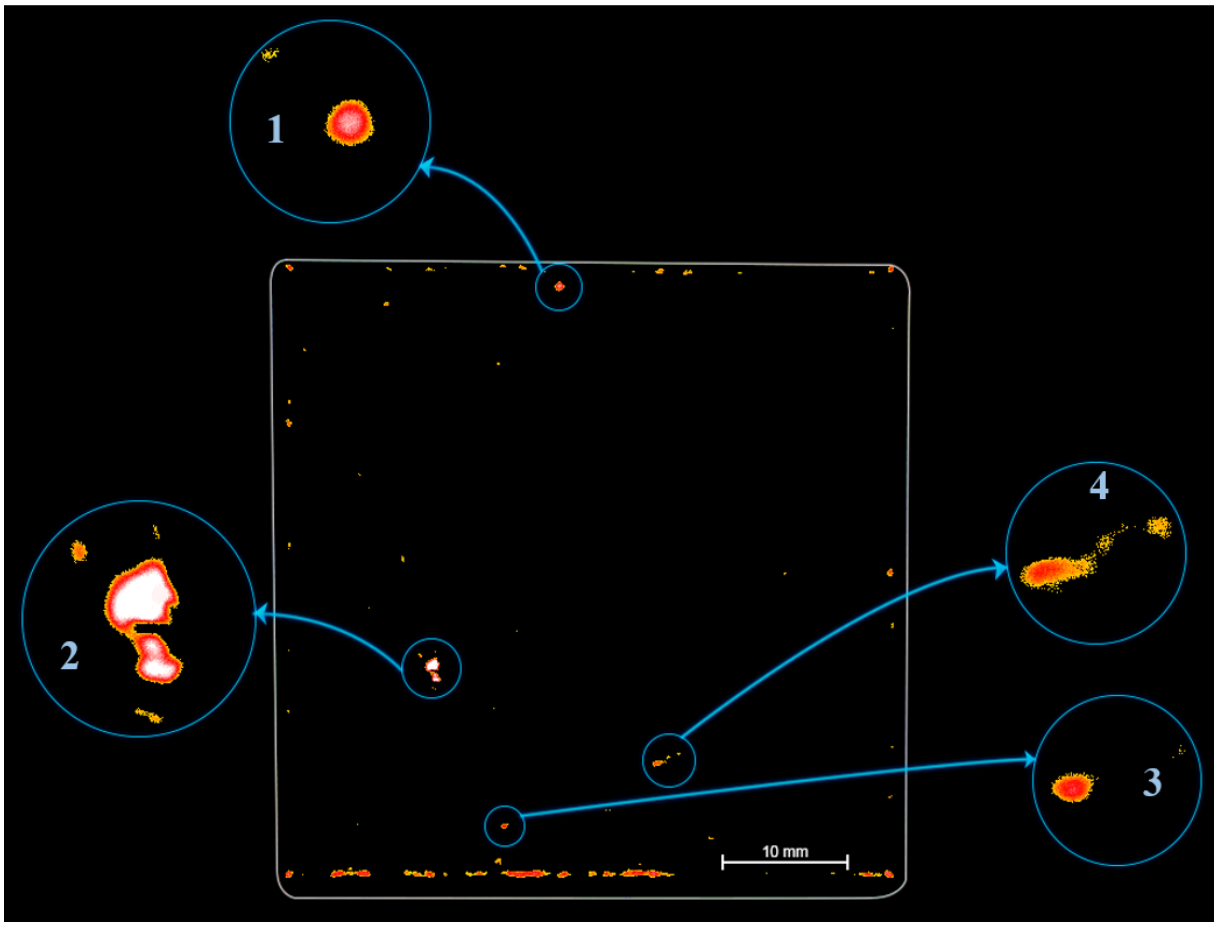


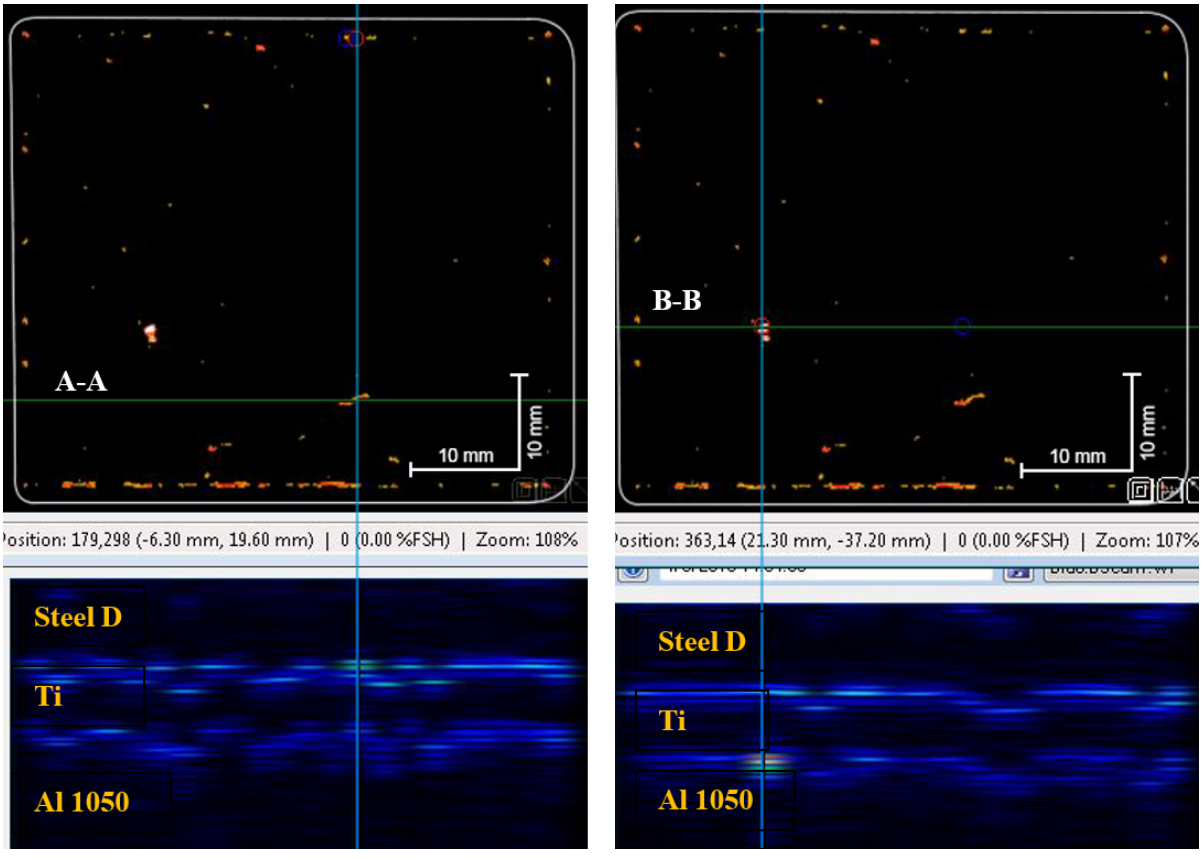
Fig. 12. Results of C-scan indications of ultrasonic tests of a four-layer clad plate: steel grade D – Ti grade 1 – Al 1050 – Al 5083. Close-ups of particular indications: (1) surface 0.44 mm^2, (2) surface 1.51 mm^2, (3) surface 0.27 mm^2 and (4) surface 0.52 mm^2

and $AlTi_3$. In remeltings also cracks were observed [55]. They were always limited to the remelted zone, which was commonly observed in other joint systems, e.g. in [56–58]. None of these cracks tended to propagate in the transverse plane of the base material [55].

In the Al 1050 and Al 5083 joint, no remeltings or adiabatic shear lines were observed (Figures 11E and 11F). On the other hand, there were large inclusions, especially at the Al 1050 side, most probably they were created as a result of local element diffusion (Figure 11F). However, the obtained joint was not wavy. The wavy profile is the preferred one as it increases the bond area and leads to a higher depth of impact hardening. This also contributes to the isolation of the trapped stream, which in turn results in the creation of an isolated mixing zone before each wave.

The SAM testing of a four-layer clad plate: steel grade D – Ti grade 1 – Al 1050 – Al 5083 was conducted form the steel grade D side. Figure 12 presents an acoustical C-Scan cross-section wide enough to overlap all three joint boundaries. The conducted tests of the analysed joints allowed the indications of the presence of possible discontinuities and imperfections to be found. Four largest discontinuities with the following dimensions: 1 – 0.44 mm^2, 2 – 1.51 mm^2, 3 – 0.27 mm^2, 4 – 0.52 mm^2, were marked.

For the selected scanning lines, Figures 13A and 13B show a B-scan presentation overlapping the boundaries of steel grade D – Ti grade 1 and



(A) (B)

Fig. 13. Results of C-scan and B-scan indications of ultrasonic tests of a four-layer clad plate: steel grade D – Ti grade 1 – Al 1050 – Al 5083 for two selected scanning lines (in both cases steel grade D – Ti grade 1 – Al 1050 are visible): **(A)** cross section A–A and **(B)** cross section B–B

Ti grade 1 – Al 1050. The visible indications may originate from voids and remeltings observed during metallographic analyses. Figure 14 shows a set of X-scan presentations at the depths corresponding to the Ti – Al 1050 boundaries in the range of 11.90–11.95 mm.

4. Discussion

SAM is a relatively new measurement technology field offering ample opportunities for the non-destructive evaluation of joints. Literature studies show that its ability to assess explosively welded joints has not been used to its full capacity, hence this study makes an attempt to make a step forward in this respect. One of the goals of the conducted research was the presentation of the SAM as an alternative to the measurement technology of metallographic tests, allowing the detection of imperfections in explosively welded joints.

First and foremost, it should be emphasised that the results obtained during the tests using SAM indicate that they are strongly influenced by the SAM ultrasonic measurement system parameters. This is why, due to the different material properties, and hence also the acoustical ones of the analysed joints, the SAM system parameters were individually set for each sample set, e.g., gain and registration threshold (the parameters were defined by the ISO 11666:2011 and PN-EN ISO 17640:2011 standards). It should also be emphasised that the tests were performed using focused beam transducers, not accounted for in the standardisation documentation. The detailed procedure of selecting mea-

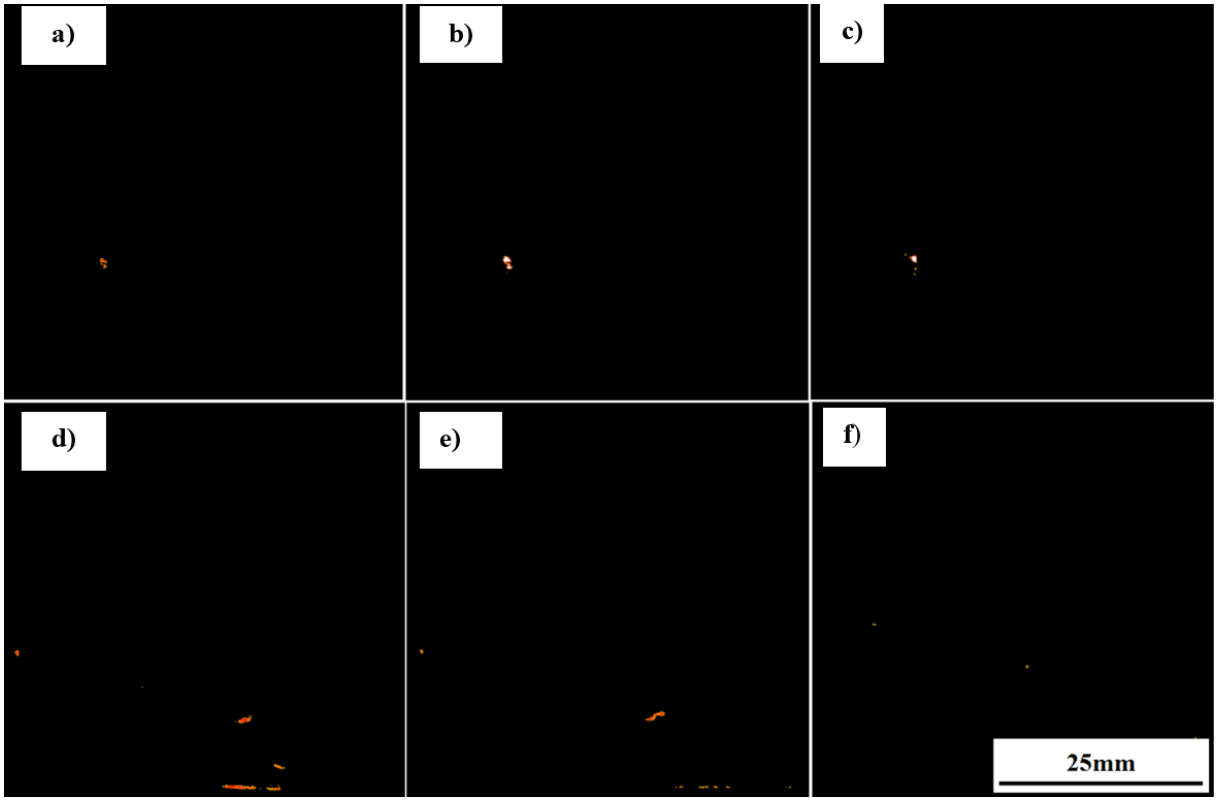


Fig. 14. A four-layer clad plate: steel grade D – Ti grade 1 – Al 1050 – Al 5083, X-scan: **(A)** depth 11.90 mm, **(B)** depth 11.91 mm, **(C)** depth 11.92 mm, **(D)** depth 11.93 mm, **(E)** depth 11.94 mm and **(F)** depth 11.95 mm, scanning acoustic microscope

surement parameters is presented with the example of the SAF 2507 – P355NH bimetal. In the case of the remaining configurations, the selection of gain settings and registration thresholds was performed in an analogous way.

4.1. SAF 2507 – P355NH

The results of ultrasonic tests in the form of a C-scan presentation and selected B-scan presentations of the SAF 2507 – P355NH bimetal show that at the joint line there are numerous indications confirming the existence of differences in the acoustic impedances of media the wave passes through. The metallographic tests of the SAF 2507 – P355NH metal revealed the presence of adiabatic shear bands and remeltings, whose presence was confirmed during the SAM tests. It should be emphasised that in the area analysed with SAM (about 2500 mm^2), the summary area with indications above the registration level was $<0.15\%$ of the total sample area (Figure 4), which in practice does not have an impact on the mechanical properties of the joint.

4.2. Inconel 625 – P355NH

The results of ultrasonic tests in the form of a C-scan presentation and selected B-scan presentations of the Inconel 625 – P355NH bimetal show that at the joint boundary there are significantly fewer indications confirming the differences in the acoustic impedances of media than in the case of the SAF 2507 – P355NH joint. Similar to the SAF 2507 – P355NH bimetal, in the Inconel 625 – P355NH joint, tests revealed the presence of adiabatic shear bands and remeltings; however, their number is considerably lower in comparison with the SAF 2507 – P355NH bimetal. SAM tests confirmed it and showed that the percentage inherence

of discontinuities was considerably <0.01% (Figure 8), which in practice does not have an adverse effect on the strength properties of the analysed joint.

4.3. Steel grade D – Ti grade 1 – Al 1050 – Al 5083

Clad steel grade D – Ti grade 1 – Al 1050 – Al 5083, due to three joint boundaries and four different materials with various acoustic properties, required particular attention. It should be mentioned that the differences in the acoustic impedances of the Al 1050 and Al 5083 alloy were not different enough that on their boundary no reflection was observed. Clear boundaries (visible in the B-scan presentation) occur at the boundary of steel grade D – Ti grade 1 and Ti grade 1 – Al 1050. The ultrasonic tests using SAM indicated the presence of discontinuities, resulting from the differences in the acoustic impedances of media. It should be mentioned that the B-scan presentation (Figure 13) allows detailed information about the depth where material discontinuities occurred to be obtained. Figure 13A shows a discontinuity which occurred at the steel grade D – Ti grade 1 border, and Figure 13B – the one on the Ti grade 1 – Al 1050 border. The metallographic tests revealed inhomogeneities near the joints which, similar to the previously analysed samples, are the places where the adiabatic shear bands and remeltings occur. The analysis of the C-scan presentation (Figure 12), overlapping three joint boundaries, indicated that the percentage participation of discontinuities in the analysed sample was about 0.2%; therefore, in practice it does not influence the mechanical properties of the clad plate. Horizontal, linear indications, visible in the bottom part of the C-scan (Figure 12) visualises discontinuities originating from the cut place of the sample and are negligible.

The formation mechanism of a durable joint as a result of an impact wave occurring during the explosive welding process implies the creation of waviness at the joint. It should also be mentioned that during the longitudinal wave ultrasonic testing, when the wave is perpendicular to the examined surface, the highest efficiency of the reflected signal registration is obtained when it is reflected from a discontinuity oriented perpendicularly to the direct beam. Remeltings and adiabatic shear bands, occurring in waviness areas can be oriented at an angle to the beam axis, which may result in decreasing the test sensitivity, and in an extreme case it can even disable the detection of discrepancies with normal heads of longitudinal waves.

5. Summary

The conducted research demonstrated the efficiency of SAM in the non-destructive assessment of clads made by explosive welding. The metallographic tests of all analysed cases revealed the presence of material discontinuities, which were confirmed by ultrasonic tests using SAM.

On the basis of the conducted research it was found that:

- The C-scan presentation of an ultrasonic signal can be used to visualise discontinuities occurring in explosively welded joints and their quantitative assessment.
- The B-scan presentation can be used in the assessment of the place where discontinuities occurred in explosively welded joints to accurately identify the joint line at which the discrepancy occurs.
- The X-scan presentation, being a set of C-scan presentations visualising the presence of discontinuities in a selected measurement area, can be used in the quantitative presentation of discontinuities in the joint at a given depth.
- The scanning ultrasonic microscopy can be used to assess the quality of plated joints consisting of more than two metals differing in mechanical properties.

Acknowledgements

The authors wish to thank the Explomet Company from Opole, and in particular Mr. Zygmunt Szulc, for offering them the samples on which the tests were performed.

Conflict of interest

Authors declare that they have no conflict of interest.

Ethical approval

This article does not contain any studies with human participants or animals performed by the authors.

References

[1] Hay DR. Explosive welding: applications and techniques. In: Timmerhaus KD, editor. High-pressure science and technology. New York: Springer Science+Business Media; 1979. pp. 1813–36.

[2] Deribas AA. Explosive welding, Academy of Sciences, USSR, Siberian Branch of the Russian Academy of Sciences, Siberia, Russia; 1967.

[3] US patent 3,137,937 GR Cowan, J. Douglas, A. Holtzman. "Explosive bonding" – published a patent on the explosive welding process 1960.

[4] Walczak W. Explosive welding of metals. Warsaw (in Polish): Scientific and Technical Publishing House; 1989.

[5] Han JH, Ahn JP, Shin MC. Effect of interlayer thickness on shear deformation behaviour of AA5083 aluminium alloy/SS41 steel plates manufactured by explosive welding. J Mater Sci. 2003;38(1):13–8.

[6] Balasubrahmanian V, Rathinasabapathi M, Raghukandan K. Modelling of process parameters in explosive cladding of mild steel and aluminium. J Mater Process Technol. 1997;63(1–3):83–8.

[7] Acarer M, Demir B. An investigation of mechanical and metallurgical properties of explosive welded aluminium–dual phase steel. Mater Lett. 2008;62:4158–60.

[8] Kahraman N, Gulenc B, Findik F. Joining of titanium/stainless steel by explosive welding and effect on interface. J Mater Process Technol. 2005;169(2):127–33.

[9] Mudali UK, Rao BMA, Shanmugam K, Natarajan R, Raj B. Corrosion and microstructural aspects of dissimilar joints of titanium and type 304L stainless steel. J Nucl Mater. 2003;321(1):40–8.

[10] Mousavi SAAA, Sartangi PF. Experimental investigation of explosive welding of cp-titanium/AISI 304 stainless steel. Mater Des. 2009;30(3):459–68.

[11] Akbari-Mousavi SAA, Barrett LM, Al-Hassani STS. Explosive welding of metal plates. J Mater Process Technol. 2008;202(1–3):224–39.

[12] Akbari-Mousavi SAA, Al-Hassani STS, Atkins AG. Bond strength of explosively welded specimens. Mater Des. 2008;29(7):1334–52.

[13] Manikandan P, Hokamoto K, Fujita M, Raghukandan K, Tomoshige R. Control of energetic conditions by employing interlayer of different thickness for explosive welding of titanium/304 stainless steel. J Mater Process Technol. 2008;195(1–3):232–40.

[14] Ege ES, Inal OT, Zimmerly CA. Response surface study on production of explosively-welded aluminum–titanium laminates. J Mater Sci. 1998;33:5327–38.

[15] Mousavi SAA, Sartangi PF. Effect of post-weld heat treatment on the interface microstructure of explosively welded titanium–stainless steel composite. Mater Sci Eng A. 2008;494(1–2):329–36.

[16] Gerland M, Presles HN, Guin JP, Bertheau D. Explosive cladding of a thin Ni-film to an aluminium alloy. Mater Sci Eng A. 2000;280(2):311–9.

[17] Livne Z, Munitz A. Characterization of explosively bonded iron and copper plates. J Mater Sci. 1987;22:1495–500.

[18] Durgutlu A, Gulenc B, Fındık F. Examination of copper/stainless steel joints formed by explosive welding. Mater Des. 2005;26(6):497–507.

[19] Kahraman N, Gulenc B. Microstructural and mechanical properties of Cu–Ti plates bonded through explosive welding process. J Mater Process Technol. 2005;169(1):67–71.

[20] Raghukandan K. Analysis of the explosive cladding of Cu–low carbon steel plates. J Mater Process Technol. 2003;139(1–3):573–7.

[21] Belyakov VA, Fabritsiev SA, Mazul IV, Rowcliffe AF. Status of international collaborative efforts on selected. J Nucl Mater. 2000;283–287(2):962–7.

[22] Tavassoli F. Overview of advanced techniques for fabrication and testing of ITER multilayer plasma facing walls. Fusion Eng Des. 1998;39–40:189–200.

[23] Durgutlu A, Okuyucu H, Gulenc B. Investigation of effect of the stand-off distance on interface characteristics of explosively welded copper and stainless steel. Mater Des. 2008;29(7):1480–4.

[24] Wronka B. Testing of explosive welding and welded joints. The microstructure of explosive welded joints and their mechanical properties. J Mater Sci. 2010;45(13):3465–9.

[25] Mamalis AG, Szalay A, Vaxevanidis NM, Manolakos DE. Fabrication of bimetallic rods by explosive cladding and warm extrusion. J Mater Process Technol. 1998;83(1–3):48–53.

[26] Ashani JZ, Bagheri SM. Explosive scarf welding of aluminum to copper plates and their interface properties. Materwiss Werksttech. 2009;40(9):690–8.

[27] Gulenc B. Investigation of interface properties and weldability of aluminium and copper plates by explosive welding method. Mater Des. 2008;29(1):275–8.

[28] Kawamura Y. Liquid phase and supercooled liquid phase welding of bulk metallic glasses. Mater Sci Eng A. 2004;375(1):112–9.

[29] Hokamoto K, Nakata K, Mori A, Ii S, Tomoshige R, Tsuda S, et al. Microstructural characterization of explosively welded rapidly solidified foil and stainless steel plate through the acceleration employing underwater shock wave. J Alloys Compd. 2009;485(1–2):817–21.

[30] Liu WD, Liu KX, Chen QY, Wang JT, Yan HH, Li XJ. Metallic glass coating on metals plate by adjusted explosive welding technique. Appl Surf Sci. 2009;255(23):9343–7.

[31] Findik F. Recent developments in explosive welding. Mater Des. 2011;32(3):1081–93.

[32] Gloc M, Wachowski M, Plocinski T, Kurzydlowski

KJ. Microstructural and microanalysis investigations of bond titanium grade1/low alloy steel st52-3N obtained by explosive welding. J Alloys Compd. 2016;671(C):446–51.
[33] El-Sobky H. Mechanics of explosive welding. In: Blazynski TZ, editor. Explosive welding, forming and compaction. Dordrecht: Springer; 1983. pp 189–217.
[34] Walczak W, Czajkowski H. Explosive welding of metals. Warsaw (in Polish): Scientific and Technical Publishing House; 1970.
[35] Wronka B. Ultrasonic flaw detection for quality assessment of explosively clad plates. Adv Mater Sci Eng. 2014; https://doi.org/10.1155/2014/171279.
[36] Kuz'min EV, Kuz'min SV, Lysak VI, Lata AN. Plastic deformation and wave formation on the interface of metals welded by ultrasonic-assisted explosive welding. J Phys Conf Ser. 2017;894(1):012047.
[37] Yu H. Scanning acoustic microscopy for material evaluation. Appl Microsc. 2020;50:25.
[38] Behrens BA, Maier HJ, Poll G, Overmeyer L, Wester H, Uhe J, et al. Influence of degree of deformation on welding pore reduction. Prod Eng. 2021;15:161–168.
[39] Xiao Z, Zeng K, He X, Zhang L. Fatigue strength and failure analysis of weld-bonded joint of stainless steel. J Adhes. 2019;95(3):187–203.
[40] Kubit T, Trzepiecinski T, Faes K, Drabczyk M, Bochnowski W, Korzeniowski M. Analysis of the effect of structural defects on the fatigue strength of RFSSW joints using C-scan scanning acoustic microscopy and SEM. Fatigue Fract Eng Mater Struct. 2019;42(6):1308–1321.
[41] Li M, Li X, Gao Ch, Song Y. Acoustic microscopy signal processing method for detecting near-surface defects in metal materials. NDT E Int. 2019;103:130–44.
[42] Zhua Y, Wanga L, Behnamianb Y, Songa S, Wanga R, Gaoa Z, et al. Metal pitting corrosion characterized by scanning acoustic microscopy and binary image processing. Corros Sci. 2020;170:108685.
[43] Pitta Bauermann L, Mesquita LV, Bischoff C, Drews M, Fitz O, Heuer A, et al. Scanning acoustic microscopy as a non-destructive imaging tool to localize defects inside battery cells. J Power Sources. 2020;6:100035.
[44] Arakawa M, Kanaiba H, Ishikawa K, Nagaoka R, Kobayashi K, Saijo Y. A method for the design of ultrasonic devices for scanning acoustic microscopy using impulsive signals. Ultrasonics. 2018;84:172–9.
[45] Ahsan Q, Kato H. Ultrasonic evaluation at the interface of aluminum/steel. IOP Conf Series: Mater Sci Eng. 2019;554:012010.
[46] Coleman BD, Hodgdon ML. On the localization of strain shearing motions of ductile materials. Res Mechanica. 1988;23(2):223–38.
[47] Magier M. The role of adiabatic shear bands effect in penetration process. Issues of Armament Technology. 2018;147(3):7–17.
[48] Rajani HRZ, Mousavi SAAA. The role of impact energy in failure of explosive cladding of inconel 625 and steel. J Fail Anal Prev. 2012;12(6); https://doi.org/10.1007/s11668-012-9601-1.
[49] Coleman BD, Hodgdon ML. On shear bands inductile materials, Analysis and Thermomechanics. Berlin: Springer; 1987.
[50] Kosturek R, Wachowski M, Śnieżek L, Gloc M. The influence of the post-weld heat treatment on the microstructure of inconel 625/carbon steel bimetal joint obtained by explosive welding. Metals. 2019;9:246–61.
[51] Chu Q, Tong X, Xu S, Zhang M, Li J, Yan F, et al. Interfacial investigation of explosion-welded titanium/steel bimetallic plates. J Mater Eng Perform. 2020;29:78–86.
[52] Nishida M, Chiba A, Honda Y, Hirazumi J-I, Horikiri K. Electron microscopy studies of bonding interface in explosively welded Ti/steel clads. ISIJ Int. 1995;35(2):217–9.
[53] Paul H, Morgiel J, Baudin T, Brisset F, Prazmowski M, Miszczyk M. Characterization of explosive welded joints by TEM and SEM/EBSD. Arch Metall Mater. 2014;59(3):1129–36.
[54] Guo Y, Bataev I, Georgarakis K, Jorge AM, Nogueira RP, Pons M, et al. Ni- and Cu-free Ti-based metallic glasses with potential biomedical application. Intermetallics. 2015;63:86–96.
[55] Paul H, Maj Ł, Prażmowski M, Gałka A, Miszczyk M, Petrzak P. Microstructure and mechanical properties of multi-layered Al/Ti composites produced by explosive welding. 17th International Conference on Metal Forming, Metal Forming 2018, 16–19 September 2018, Toyohashi, Japan; 2018.
[56] Paul H, Lityńska-Dobrzyńska L, Prażmowski M. Microstructure and phase constitution near the interface of explosively welded aluminium/copper plates. Metall Mater Trans A. 2013;44A:3836–51.
[57] Paul H, Morgiel J, Faryna M, Prażmowski M, Miszczyk MM. Microstructure and interfacial reactions in the bonding zone of explosively welded Zr700 and carbon steel plates. Int J Mater Res. 2015;106:782–92.
[58] Paul H. Interfacial reactions during explosive bonding. Mater Sci Forum. 2014;783–786:1476–81.

Received 2022-12-13
Accepted 2022-12-21